P3.3 THE HISTORIC MISSOURI-ILLINOIS HIGH PRECIPITATION SUPERCELL OF 10 APRIL 2001

Fred H. Glass* and Mark F. Britt

NOAA/National Weather Service
St. Charles, Missouri

1. INTRODUCTION

During the afternoon and evening hours of 10 April 2001 a devastating long-lived high precipitation (HP) supercell traversed Missouri and southwest Illinois. This single storm produced nine weak tornadoes during it's 5.5 hour life span. All of the tornadoes were rated F0-F1 with path lengths varying from 5-10 miles for the first three tornadoes to 1-4 miles for the later five. There was also a brief touchdown of an apparent non-supercell tornado in Moniteau County, southwest of Columbia (COU). The F1 tornado which struck Fulton (southeast of COU) destroyed a mobile home producing the first tornado fatality in Missouri since 1994. Eyewitness accounts indicate most of the tornadoes were rain-wrapped and not visible; consistent with the HP theme. Total cumulative damage from the tornadoes was around 12 million dollars.

While the spawning of nine tornadoes alone is noteworthy, the HP supercell will long be remembered for its prolific hail production. The storm produced a swath of large hail nearly 470 km in length and 30-50 km in width as it moved east through the highly-populated Interstate-70 corridor from Kansas City through St. Louis, resulting in hail damage of historic proportions. Most of the hail ranged in size from golfball to baseball (1.75-2.75 in/4.45-7.00 cm). Insurance claims to date are at 1.4 billion dollars for the hail alone, consisting of over 65,000 claims for automobiles, 100,000 for homes, and 6,000 for commercial losses. This figure does not include a number of private and commercial loses, including damage to hundreds of SUVs at the Ford Motor Company Plant in St. Louis County and tens of commercial and military aircraft at Lambert St. Louis International Airport. A map documenting the tornado tracks and large hail swath is shown in Fig. 1. The losses make this HP supercell one of the costliest hailstorms to date in U.S. History, second only to the Mayfest Storm of May 1995 in Dallas.

An intensive, detailed analysis of this event is not possible due to space limitations. Therefore the information presented highlights significant observations from the course of our research. In this paper we review: 1) the role of a preexisting outflow boundary and mesolow in the development and evolution of the HP storm, 2) the development of the HP storm and its continually evolving structure as viewed from WSR-88D radars in Pleasant Hill (EAX) and St. Louis (LSX), 3) the multiple updraft structure, 4) the cyclic mesocyclone production, and 5) presence of several tornado cyclones.

2. MESOSCALE FEATURES

The upper-air data from 1200 UTC 10 April 2001 and 0000 UTC 11 April 2001 *(hereafter all times are UTC and year 2001; times after 0000 correspond to 11 April)* and intermediate surface datasets showed moisture, instability, and shear stratifications supportive of organized convective storms including severe storms over much of the central Plains and mid-Mississippi Valley. While these conditions were present over a large region, the most favorable conditions for surface-based severe storms were in the vicinity of a stationary front draped across Kansas and southward into the warm sector, and near and south of an old large-scale convective outflow boundary which stretched west-east from eastern Kansas through central Missouri into the lower Ohio Valley.

The preexisting outflow boundary and an apparent storm-induced mesolow were key factors modulating supercell development, evolution, storm motion, longevity, and tornado production. The development of the HP supercell (see also section 3) resulted from the merger of two northeast-moving classic supercell thunderstorms which attained their rotation immediately after crossing the surface outflow boundary. Following the merger, the resultant HP storm deviated to the right as it became "anchored" to the thermal gradient immediately on the cool side of the west-east surface boundary. The supercell then moved east along the boundary with the advancing mesolow at 45-50 mph for a 5+ hour period. Figure 2 is a surface analysis for 2300 depicting the boundary and mesolow positions almost one hour into the HP supercell's lifespan. Given the resolution of the surface data, it is difficult to conclude with total certainty, however the 8 supercell tornadoes all appear to have occurred within a 10 km zone on the cool side of the boundary.

The outflow boundary initially evolved during the early morning hours of 10 April in response to the cumulative outflow from a series of MCSs moving eastward across the Mississippi and Ohio Valleys. By mid-morning the large-scale outflow boundary extended westward from northern Kentucky across southern Illinois and southern Missouri into southeast Kansas. Despite extensive cloudiness across the region, occasional breaks in the warm sector cloud cover allowed the airmass south of the boundary to warm into the middle 70s to lower 80s (°F) by mid-afternoon. To the north of the boundary however, persistent cloud cover along with several waves of diurnal convection suppressed warming, holding temperatures in the 60s to lower 70s (°F). This differential heating maintained the structure and position of the large-scale outflow boundary and allowed it to have an increasingly frontogenetic character.

Similar to findings by Maddox (1980), the outflow boundary appeared critical organizing heat and moisture distributions in the boundary layer and the resultant stability stratifications. Surface observations at 2100 (around one hour before HP development) indicated temperatures decreased no more than 10 degrees F in a 75 km zone north of the boundary, while surface dew points actually increased and were pooled along and to the north of the boundary. This resulted in relatively small dew point depressions. The increase in dew points was

*Corresponding author address: Fred H. Glass, NOAA/NWS, 12 Research Park Drive, St. Charles, MO 63304; email: fred.glass@noaa.gov

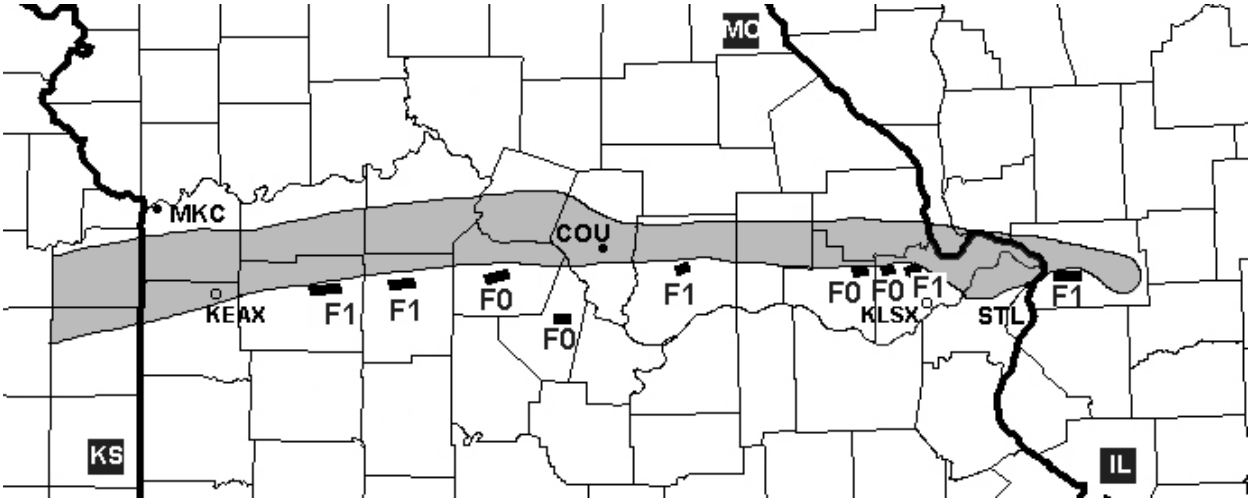

Figure 1. Map of tornado tracks (F-scale denoted) and large hail swath ($1.00 in, shaded).

possibly due to or enhanced by a shallow frontogenetical circulation, as well as moistening from the previous thunderstorms. Thus with observed mid-level lapse rates around 7.0 °C km^{-1}, surface-based instability was maintained well into the cool sector. Objective analyses using the ETA model as a background indicate surface-based CAPE (SBCAPE) of 2000-3000 J kg^{-1} in the warm sector, diminishing to only 1000-1500 J kg^{-1} as far as 75 km into the cool air north of the boundary. The aforementioned small surface dew point depressions suggested low lifting condensation levels (<2000 ft AGL). A climatological study of soundings by Rasmussen and Blanchard (1998) found a preference for low LCLs (below 800 m AGL) for strong and violent tornadoes. The 0000 11 April Topeka (TOP) sounding *(not shown),* located approximately 30 km north of western periphery of the boundary confirmed the presence of low LCLs with a value of around 1400 ft AGL (427 m). The boundary remained well-defined through 0200 when the HP supercell entered the immediate St. Louis Metro Area, although the loss of insolation/heating contributed to a decrease in SBCAPE to around 1000 J kg^{-1}.

The VWPs from EAX at 2131 and LSX at 0155 were examined to evaluate the character of the vertical and horizontal wind field just north of the boundary prior to the arrival of the supercell. A representative nearby surface wind was incorporated with the VWP data. Vertical profiles from both sites indicate backed flow in the lowest levels with surface winds from the east, then veering and increasing winds with height. The resultant hodographs exhibit substantial low-level cyclonic curvature/shear and significant storm-relative helicity (SRH). SRH values in the 0-3 km layer using an observed storm motion of 270°/43kts were 876 m^2 s^{-2} for EAX and 581 m^2 s^{-2} for LSX. The higher value found at EAX was the result of deeper low-level southeasterly flow and slightly greater wind speeds. These high SRH values are probably not only a reflection of the ambient environmental vorticity, but are likely augmented by horizontal baroclinic vorticity associated with the thermal gradient, and streamwise vorticity amplification due to increased inflow via the mesolow. Brooks et al. (1994) and Weisman et al. (1998) have both discussed the ramifications of accelerated inflows due to the storm itself. Observations presented herein of high SRH and storm-motion along the boundary (*a source of baroclinically generated vorticity*) are consistent with the findings of Markowski et al. (1998) and Atkins et al. (1999) favorable for low-level and mid-level mesocyclone development and enhanced tornado potential.

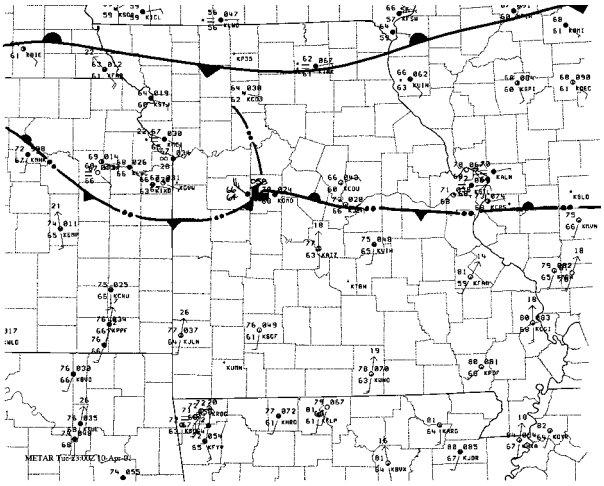

Figure 2. Surface mesoanalysis for 2300 10 April 2001.

3. STORM STRUCTURE AND EVOLUTION

A sequence of 0.5° reflectivity images from EAX and LSX are shown in Fig. 3 to help document the development and evolution of the HP supercell during a 5 hr period. The storm displays complex evolutions and reflectivity distributions akin to the conceptual model of Moller et al. (1990) and the recent observational studies of Glass and Przybylinski (1998) and Pence and Peters (2000). The series begins at 2201 (Fig. 3a) with two classic supercells over and just east of EAX. The

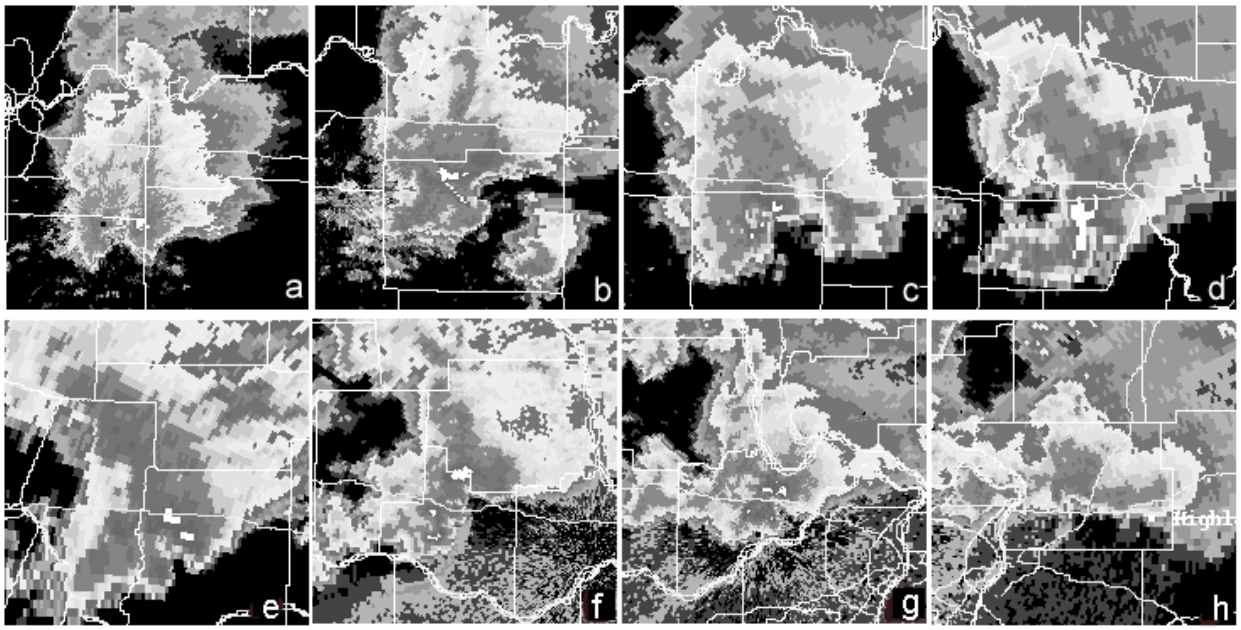

Figure 3. Sequence of 0.5° reflectivity images for a) 2201, b) 2221, c) 2301, d) 2336, e) 0013, f) 0119, g) 0155, and h) 0251.

storms are just beginning to merge, and both feature prominent appendages associated with low-level mesocyclones. By 2221 and immediately prior to the beginning of the first tornado near Warrensburg, an enlarging echo mass is apparent as the two storms continue to merge (Fig. 3b). The western supercell has taken on a bow-echo structure as its mesocyclone has translated poleward entraining low 2_e air from the west. The resultant eastward surge of the RFD accelerates the merger process and appears to enhance the RFD of the eastern supercell. Distinguishable characteristics of the eastern storm include a prominent hook echo associated with a deep and strong mesocyclone, and high reflectivities throughout the forward and rear flank regions (FFD/RFD). An isolated storm displaying weak mid-level rotation is also located southeast of the main echo mass. Figure 3c indicates the merger is complete by 2301 and the isolated thunderstorm has also merged with the echo mass on the far eastern fringes. The HP has already produced a second tornado near La Monte. The associated mesocyclone has completely redistributed the precipitation field and is completely enshrouded in higher reflectivities on the forward flank, with a new mesocyclone core just to the southeast.

By 2336 the HP continues to evolve with a psudeo-bow type structure featuring a weak echo region (WER) on the forward flank (Fig. 3d). The WER is a reflection of a new updraft and mesocyclone core which has developed on the foward southeast flank. The previous two mesocyclone cores have translated rearward and poleward, weakening and broadening in the process. The eastern-most extension of the echo mass is a reflection of the isolated storm merger which has translated northward. Figure 3e from 0013 shows the HP supercell continues to exhibit a pseudo-bow type structure as it progresses eastward through central Missouri. A large WER and 'fat echo knob' are located on the forward southeast flank. The previous mesocyclone core has occluded to a position near the rear of the WER, while a new core has developed just north of the knob structure. Over an hour later the reflectivity structure has evolved further with a more elongated north/south reflectivity field extending south of the main low-level WER (Fig. 3f). This appears to be a reflection of a more extensive RFD region with the gust front quite apparent and emanating southward from the main WER. *(A more detailed discussion of this evolution will be presented in section 4).* High reflectivities (>65 dBz) which have been consistently observed in the forward flank region since the storm developed are still present and indicative of the large hail.

At 0155 the HP supercell is located over St. Charles County and just north of the LSX WSR-88D (Fig. 3g). The southward extension of reflectivity seen in Fig. 3f is no longer apparent, however there is considerable precipitation extending westward from the forward storm flank. A new mesocyclone is coincident with the WER just northeast of the radar, while the older mesocyclone core has translated poleward and is embedded well into the higher reflectivies at the rear of the storm (north-northwest of the radar). Figure 3h indicates the appearance of the storm has changed considerably by 0251, not even one hour later. The storm motion slowed during this period and now the storm reflectivity and velocity pattern is that of a classic supercell with a single mesocyclone on the southwest flank. Structurally, compared to the evolution in the preceding 5 hours, the storm is now smaller and shallower, while the associated mesocyclone (which has just produced the final tornado) is smaller and weaker. The supercell continues to weaken as it moves eastward, dissipating by 0330.

4. UPDRAFT STRUCTURE

Nelson and Knight (1987) and Nelson (1987) documented what they termed a hybrid multicellular-supercellular to describe a severe hailstorm which had supercell characteristics but possessed multiple updraft

centers within a larger updraft region. Under today's nomenclature this would be termed a high precipitation supercell. Our storm possessed many of the traits of the 'Nelson storm' including a large updraft current, extending over 10km downwind of the low-level reflectivity gradient, with embedded intense rotating updraft centers. This structure was very persistent through the life of the storm. Figure 4 illustrates this structure early on, displaying multiple mid-level BWERs when the storm is 20 nm east of EAX. A cross-section taken parallel to the low-level inflow region (Fig. 5a) nearly 2.5 hrs later shows a similar structure. The reflectivity cross section in Fig. 5b shows two discrete intense updraft centers within a large updraft current. The velocity cross section in Fig. 5c confirms these updrafts are rotating (ie. mesocyclones aloft).

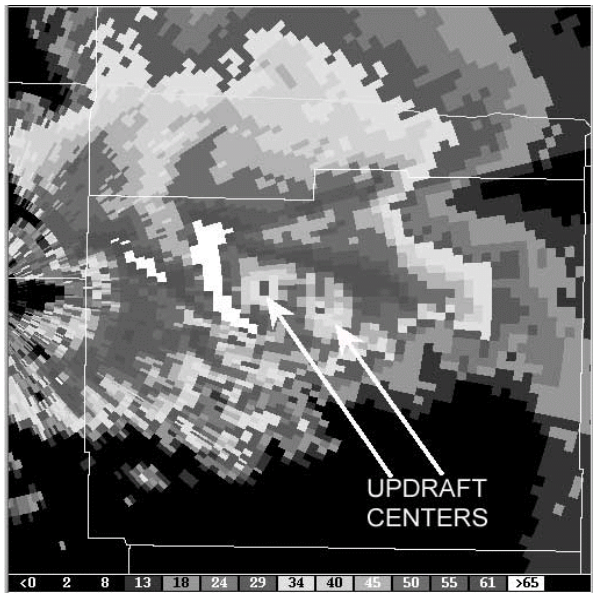

Figure 4. EAX 8.7° reflectivity image at 2214 (18.0 kft).

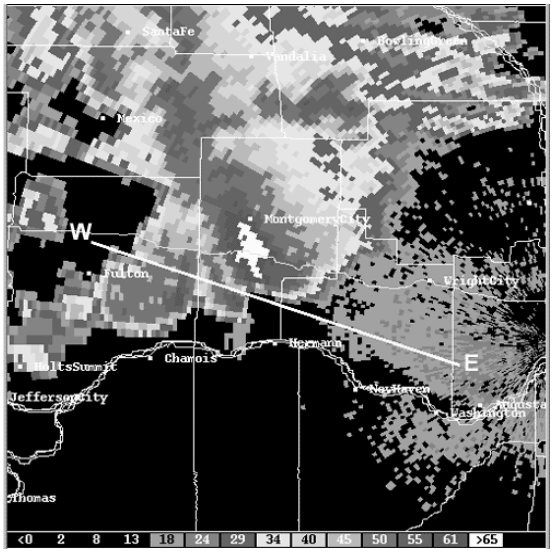

Figure 5a. LSX 0.5° reflectivity image at 0048 depicting the W-E cross section shown in (b) and (c).

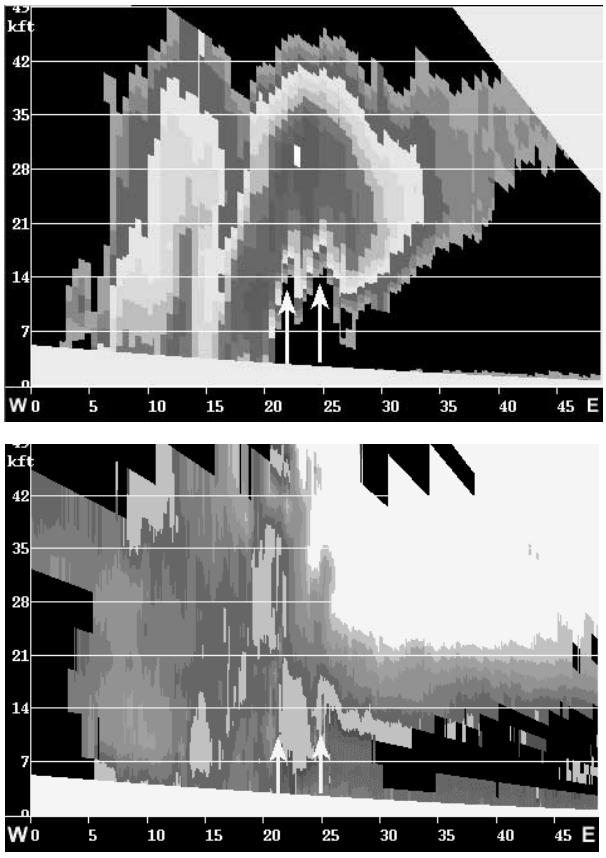

Figure 5b (top) reflectivity cross-section, and 5c (bottom) velocity cross section. Vertical scale is kft ARL.

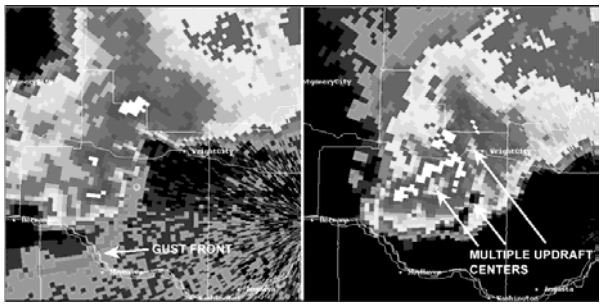

Figure 6. LSX reflectivity images for 0118 at 1.3 kft (left) and 16.7 kft (right).

The updraft structure within the HP changes briefly during the period from around 0100 to 0145, elongating southward in advance of an expanding rear flank precipitation region. Figure 6 depicts this orientation at 0118. The northern-most updraft center is associated with the mesocyclone while the two southern centers are located along and in advance of a prominent north-south RFD gust front. A vertical cross-section (not shown) taken orthogonal to the boundary and these southern updraft cores depict a very deep convergence zone similar to that described by Lemon and Burgess (1993). Gaddy and Bluestein (1998) found a similar structure for a severe supercell hail storm in Texas. During this period it

appeared smaller severe hail (0.75-1.00 in) formed within the broad updraft region in a manner suggested by Nelson (1983). The largest, most severe hail throughout the storm life-cycle was associated with the large updraft region on the forward flank of the supercell, with the mesocyclonic circulation distributing most of this hail in the forward flank region.

5. CYCLIC MESOCYCLONE PRODUCTION

At least 10 mesocyclone cores were observed during the lifespan of the HP supercell. The task of tracking the individual cores and the associated occlusions was quite tedious at close ranges where velocity averaging is less and where high resolution Archive II data shows considerably more detail. Smaller scale circulations were evident at times, which could be interpreted as new cores, but were more likely the smaller scale vortex termed a tornado cyclone (Agee et al. 1976). The actual cyclic mesocyclogensis process observed, conformed closely to that seen in other HP supercells by the authors and is similar to that described by Dowell and Bluestein (2000). New mesocyclone cores form to the southeast of the previous cores over a relatively deep layer along the forward flank and ahead of the low-level gust front/reflectivity appendage. The cores then mature as they translate westward through the updraft region, and then are "shed" to the rear of the storm were then broaden and weaken and eventually dissipate. The HP supercell seemed to achieve some "quasi-balance" with the environment during it's eastward track as the outflow never surged ***well in advance*** as would occur in an outflow dominated storm, and thus successive cores formed with regularity on the forward southeast flank in the vorticity rich environment.

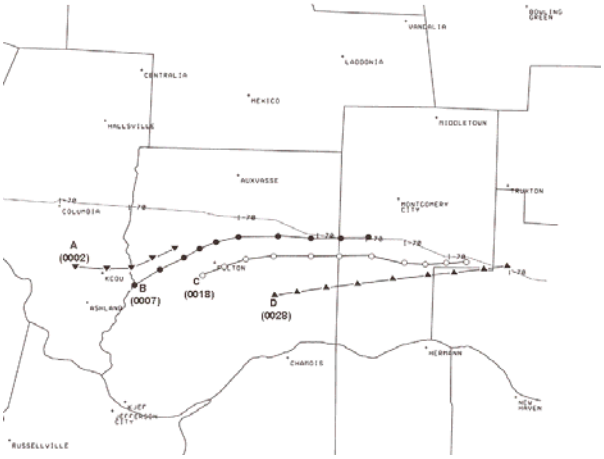

Figure 7. Low-level mesocyclone core tracks for the period from 0002-0109.

Figure 7 is a diagram of low-level mesocyclone cores observed during the period from 0002 through 0109 as the supercell moved east of Columbia. The individual mesocyclone cores A-D in the diagram all persist in excess of 45 minutes. The reflectivity and velocity images shown in Fig. 8 depict the supercell, with the co-existent multiple mesocyclone cores denoted, just prior to producing the deadly F1 tornado in Fulton. The A-C labeling of the circulations in Fig. 8b corresponds to the tracks of the same circulations shown in Fig. 7. In Fig. 8, mesocyclone core C located near the tip of the fat reflectivity knob is the newest circulation and is associated with the deadly tornado. The oldest core A can be associated to the rear of the storm in the corresponding reflectivity image.

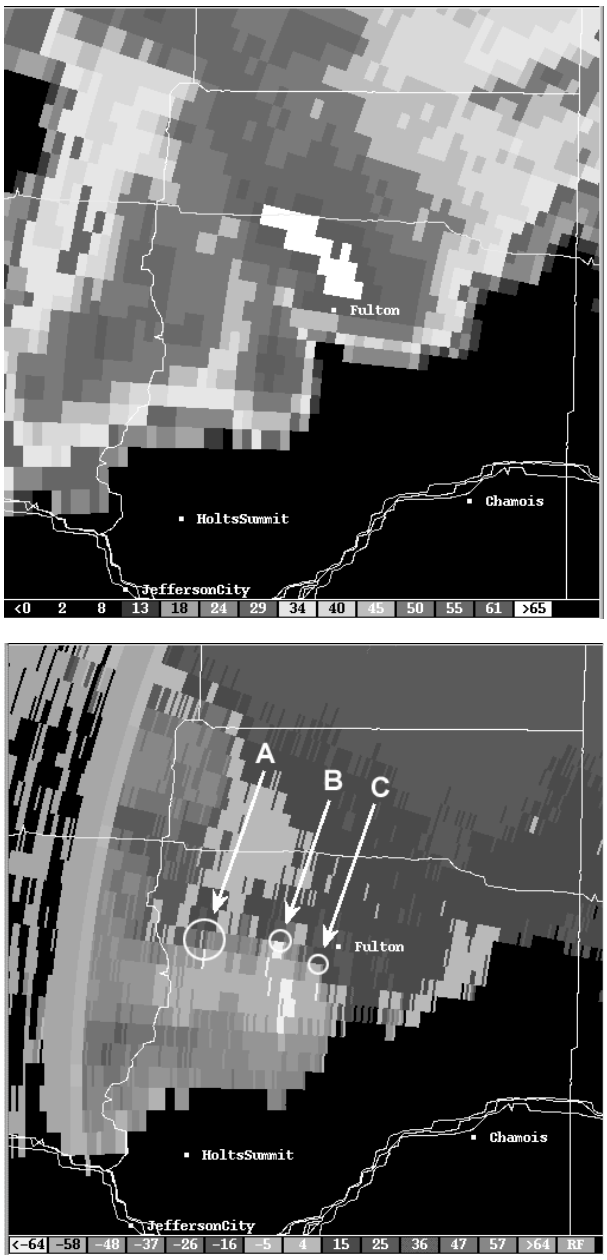

Figure 8. LSX 0.5° images at 0018 for reflectivity (top - a) and base velocity (bottom - b). Mesocyclone cores are annotated on the velocity image.

6. TORNADO CYCLONES

Agee et al. (1976) described the smaller scale vortices found within the mesocyclone circulation as *'mini'* tornado cyclones. During the course of our study we found that when

the HP supercell was at close range to the WSR-88Ds at EAX and LSX *(generally less than 30 nm)*, these smaller scale circulations were apparent at times. A total of five circulations were clearly discernable in the high resolution archive level II velocity data - all associated with tornadoes. Two of these were apparent when the storm was in close proximity to EAX, while the other three were within the LSX radar umbrella. The signatures in the velocity data varied in appearance depending on the height and range at which they were observed. Aloft and above the cloud base, the signatures were manifested as a pair of tighter velocity peaks (but not gate-to-gate) superimposed within broader velocity peaks of the mesocyclone. Figure 9 is an example of this tornado cyclone signature at a range of 19 nm and height of 7.0 kft ARL just prior to the Warrensburg tornado. Burgess and Magsig (1998) and Glass and Britt (2000) found similar patterns for small scale circulations in their close range observational studies. Below the cloud base (0.3-0.5 kft ARL) the tornado cyclone appeared to be manifested as a small diameter mesocyclone with an embedded gate-to-gate signature. An example of this profile at the time of the Lake St. Louis F1 tornado is shown in Fig. 10; the feature is just 7 nm northwest of the radar at a height of 0.5 kft ARL. Interestingly the gust front is very occluded and wrapped well into the precipitation towards the rear of the storm. Most of the tornado cyclone signatures were brief, appearing for one or two volume scans near the tornado time. The exception was the tornado cyclone signature associated with the first tornado at Warrensburg. This circulation was first evident 11 minutes (3 volume scans in VCP 11) before the tornado and remained discernable for 25 minutes.

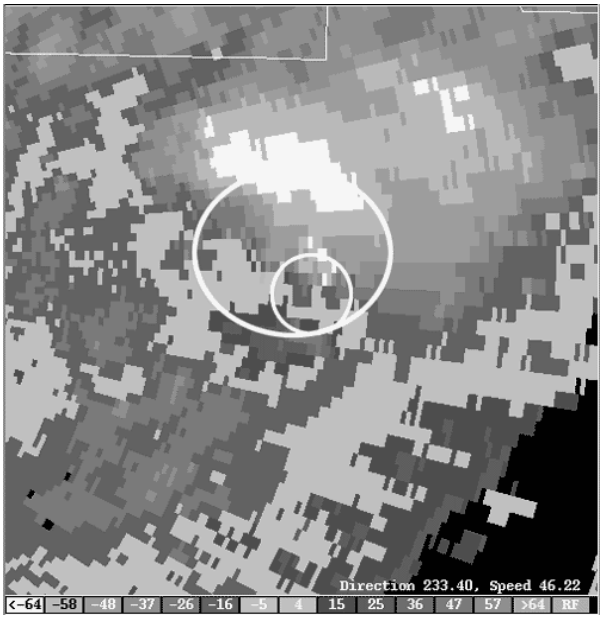

Figure 9. EAX 3.3° storm-relative velocity image for 2216. The mesocyclone is annotated with larger circle, while the tornado cyclone is annotated with the smaller circle.

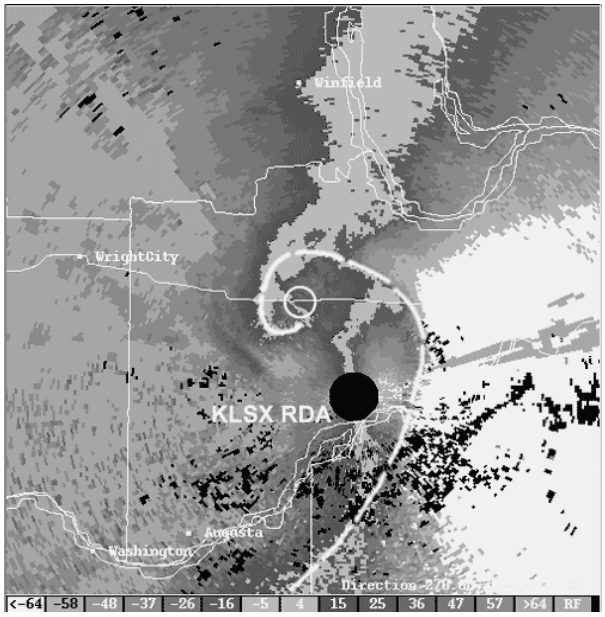

Figure 10. LSX storm-relative velocity image for 0155. Tornado cyclone denoted with small circle, while occluded RFD gust front is denoted with dashed line.

ACKNOWLEDGMENTS

We extend our thanks to the following WFO LSX personnel: Steven Thomas (MIC) for administrative support, Ron Przybylinski (SOO) for scientific support and graphics assistance, Eric Lenning (ITO) for data and software support, and Arno Perlow (DAPM) for graphics support. Lastly we thank Steve Corfidi (SPC) for some of the data used in this study.

REFERENCES

Agee, E. M., J. T. Snow, and P. R. Clare, 1976: Multiple vortex features in the tornado cyclone and the occurrence of tornado families. *Mon. Wea. Rev.*, **104**, 552-563.

Atkins, N. T., M. L. Weisman, and L. J. Wicker, 1999: The influence of preexisting boundaries on supercell evolution. *Mon. Wea. Rev.*, **127**, 2910-2927.

Brooks, H. E., C. A. Doswell III, J. Cooper, 1994: On the environments of tornadic and nontornadic mesocyclones. *Wea. Forecasting*, **9**, 606-618.

Burgess, D. W., and M. A. Magsig, 1998: Recent observations of tornado development at near range to WSR-88D radars. *Preprints, 19th Conf. on Severe Local Storms*, Minneapolis, MN., Amer. Meteor. Soc., 756-759.

Dowell, D. C., and H. B. Bluestein, 2000: Conceptual models of cyclic supercell tornadogenesis. *Preprints, 20th Conf. on Severe Local Storms*, Orlando, FL., Amer. Meteor. Soc., 259-262.

Gaddy, S. G., and H. B. Bluestein, 1998: Airborne dual-doppler analysis of a supercell hailstorm. *Preprints, 19th Conf.*

on Severe Local Storms, Minneapolis, MN., Amer. Meteor. Soc., 60-63.

Glass, F. H., and R. W. Przybylinski, 1998: Rapid evolution of a tornadic high precipitation (HP) supercell and subsequent cyclic mesocyclogenesis. *Preprints, 19th Conf. on Severe Local Storms*, Minneapolis, MN., Amer. Meteor. Soc., 200-205.

_____, and M. F. Britt, 2000: Close range observations of several tornadic storms. *Preprints, 20th Conf. on Severe Local Storms*, Orlando, FL., Amer. Meteor. Soc., 190-193.

Lemon, L. R., and D. W. Burgess, 1993: Supercell associated deep convergence zone revealed by a WSR-88D. *Preprints, 26th Inter. Conf. on Radar Meteor.*, Norman, OK., Amer. Meteor. Soc., 206-208.

Maddox, R. A., L. R. Hoxit, and C. F. Chappell, 1980: A study of tornadic thunderstorm interactions with thermal boundaries. *Mon. Wea. Rev.*, **108**, 322-336.

Markowski, P. M., E. N. Rasmussen, and J. M. Straka, 1998: The occurrence of tornadoes in supercells interacting with boundaries during VORTEX-95. *Wea. Forecasting*, **13**, 852-859.

Moller, A. R., C. A. Doswell III, and R. Przybylinski, 1990: High-precipitation supercells: A conceptual model and documentation. *Preprints, 16th Conf. on Severe Local Storms*, Kananaskis Park, Alta., Canada, Amer. Meteor. Soc., 52-57.

Nelson, S. P., 1983: The influence of storm flow structure on hail growth. J. Atmos. Sci., **40**, 1965-1983.

_____, and N. C. Knight, 1987: The hybrid multicellular-supercellular storm-an efficient hail producer. Part I: An archetypal example. *J. Atmos. Sci.*, **44**, 2042-2059.

_____, 1987: The hybrid multicellular-supercellular storm-an efficient hail producer. Part II: General characteristics and implications for hail growth. *J. Atmos. Sci.*, **44**, 2060-2073.

Pence, K. J., and B. E. Peters, 2000: The tornadic supercell of 8 April 1998 across Alabama and Georgia. *Preprints, 20th Conf. on Severe Local Storms*, Orlando, FL., Amer. Meteor. Soc., 206-209.

Rasmussen, E. N., and D. O. Blanchard, 1998: A baseline climatology of sounding-derived supercell and tornado forecast parameters. *Wea. Forecasting*, **13**, 1148-1164.

Weisman, M. L., M. S. Gilmore, and L. J. Wicker, 1998: The impact of convective storms on their local environment: What is an appropriate ambient sounding? *Preprints, 19th Conf. on Severe Local Storms*, Minneapolis, MN., Amer. Meteor. Soc., 238-241.